USING THE DYNAMIC PLATFORM FOR THE DETECTION OF CANCER BIOMARKER CD44

Zhuldyz Myrkhiyeva

BSc in Pharmacology, King's College London

Submitted in fulfillment of the requirements

for the degree of Master of Science

in Biomedical Engineering

School of Engineering and Digital Sciences
Department of Chemical & Materials Engineering
Nazarbayev University

53 Kabanbay Batyr Avenue,

Nur-Sultan, Kazakhstan, 010000

Supervisor: Daniele Tosi

Co-supervisor: Chang-Keun Lim

Date: April 2023

DECLARATION

I hereby declare that the thesis is my original work and it has been written by me in its entirety. I have duly acknowledged all the sources of information which have been used in the thesis. This thesis has also not been submitted for any degree in any university previously.

Zhuldyz Myrkhiyeva

April 2023

ACKNOWLEDGEMENTS

All praise to Allah for giving me the strength and wisdom to achieve one of my goals. First of all, I would like to express my gratitude to my advisor, Professor Daniele Tosi, for giving me the opportunity to conduct research in his lab and for his guidance throughout my research. Sincerely appreciate Dr. Aliya Bekmurzayeva's advice, direction, and encouragement whenever I needed it. I would like to give a special thanks to all my laboratory mates who helped me during my experiments. Most importantly, I would like to express my deepest gratitude to my parents, sisters, children and my husband for their support and love.

TABLE OF CONTENTS

ABSTRACT

Early detection of CD44 cancer biomarker is essential because overexpression of the transmembrane protein CD44 in the human body is a signal for the growth and progression of tumors. Clinical studies confirmed that CD44 is considered useful in prognozing and diagnosing several types of cancer, such as gastric, colon, breast and oral cancer. Therefore, accurate and easy-to-use CD44 biomarker detection methods can significantly assist in cancer diagnosis and control disease conditions. This conducted study aims to develop an accurate dynamic biosensing platform for detecting CD44 biomarker to mimic blood flow, thus allowing to move one step closer to the clinical application. *In vitro* studies were done after optimizing the dynamic setup, and sucrose solution measurement was performed in static and dynamic conditions to see the difference and resolve issues before protein measurement. SMF-28 fibers were utilized to manufacture optical fiber ball resonators in the lab, and these fabricated optical fiber ball resonator biosensors were designed to detect CD44 protein. CD44 protein detection and specificity tests were done with several functionalized biosensors in dynamic conditions. Developed optical fiber biosensor demonstrated its competence in the detection of CD44 biomarker.

KEYWORDS optical fiber biosensor, CD44, biomarker, biosensor, biomarker detection

List of Abbreviations & Symbols

FOS	Fiber Optic Sensor
OBR	Optical Backscatter Reflectometry
AFM	Atomic Force Microscopy
RI	Refractive index
CD44	Cluster differentiation 44
ELISA	Enzyme-linked immunosorbent assay
FPS	Fiber Processing Software
SMF-28	Single mode fiber-28
PBS	Phosphate buffer solution
DI	Deionized
APTMS	3-aminopropyl trimethoxysilane

List of Tables

List of Figures

List of publications

1) Zhannat Ashikbayeva, Aliya Bekmurzayeva, **Zhuldyz Myrkhiyeva**, Nazerke Assylbekova, Timur Sh.Atabaev, DanieleTosi. “Green-synthesized gold nanoparticle-based optical fiber ball resonator biosensor for cancer biomarker detection”. Optics & Laser Technology, 161, 1091136, **2023**.
2) Aliya Bekmurzayeva, Zhannat Ashikbayeva, Nazerke Assylbekova, **Zhuldyz Myrkhiyeva**, Ayazhan Dauletova, Takhmina Ayupova, Madina Shaimerdenova, Daniele Tosi. “Ultra-wide, attomolar-level limit detection of CD44 biomarker with a silanized optical fiber biosensor”. Biosensors and Bioelectronics, 208, 114217, **2022**
3) Aliya Bekmurzayeva, Zhannat Ashikbayeva, **Zhuldyz Myrkhiyeva**, Aigerim Nugmanova, Madina Shaimerdenova, Takhmina Ayupova, Daniele Tosi. "Label-free fiber-optic spherical tip biosensor to enable picomolar-level detection of CD44 protein." Scientific reports 11 (1), 19583, **2021**
4) Daniele Tosi, Zhannat Ashikbayeva, Aliya Bekmurzayeva, **Zhuldyz Myrkhiyeva**, Aida Rakhimbekova, Takhmina Ayupova, Madina Shaimerdenova. "Optical fiber ball resonator sensor spectral interrogation through undersampled klt: Application to refractive index sensing and cancer biomarker biosensing." Sensors 21 (20), 6721, **2021**

Chapter 1 – Introduction

1.1 Problem/area of application

Cancer continues to pose a formidable problem around the world despite significant medical advances. This has led to an increasing study and literature that emphasizes that cancer diagnosis in the early stage has an essential impact on the positive outcome of the treatment. As defined by Camerlingo et al. (2013), cancer is the active, progressive growth of atypical cells that replace normal tissue. A cancer diagnosis is based on symptoms, but symptoms tend to appear at a late stage of the disease. The World Health Organization reports that one out of six deaths worldwide occurs because of cancer. Cancer mortality and morbidity are primarily caused by metastases, and one of the few proteins that play a significant role in metastasis is CD44 [1].

Cluster differentiation 44 (CD44) protein is a transmembrane glycoprotein with roles in cell division, migration, adhesion, and signaling. The expression of CD44 is found in many cell types, and the molecular weight of CD44 is around 85-200KDa [2]. CD44 has a role in physiological processes, and numerous studies have reported a link between CD44 protein and cancer development. As a result of its interaction with its ligand, CD44 plays a pivotal role in carcinogenesis by regulating cell adhesion, motility, matrix degradation, proliferation, and survival of cells [3]. Numerous studies confirmed the oncogenic properties of CD44 protein and labelled it as a cancer biomarker. The term 'biomarker' refers to a measurable biological process used to indicate disease risk or health status [13]. CD44 serves as a surface biomarker that promotes the proliferation of cancer stem cells that lead to metastasis. Through activating various signaling

pathways, CD44 is responsible for stimulating epithelial-mesenchymal transition, which causes the cell to invade and spread cancer [5].

Recently, cancer detection methods that do not require invasive procedures have increasingly relied on the CD44 protein. In terms of affordability and ease of use, the current commercially available methods for detecting CD44 protein have drawbacks such as not being label-free, long hours of detection, and not being applicable for *in vivo* use due to electromagnetic interference. Using biomarkers to detect cancer has been gaining popularity due to recent developments in the field of biosensors. At present, several methods are available for detecting CD44, including photoelectrochemical (PEC) technologies with antifouling interface biosensors, fluorescence assays, and enzyme-linked immunosorbent assays (ELISA). The ongoing project for developing biosensors includes the features of two different photo- and electrochemical detection methods of biomolecules [6]. This method is distinguished by the simplicity of its development and usage, as well as the equally important fact that it is antibody-free [6]. The authors also claim that the biosensor has good antifouling properties by testing it in IgG and PSA as biofouling agents. They believe that hybrid coating of biosensors makes it possible to compromise in terms of antifouling and selective detection of CD44 protein. Another platform for CD44 is ELISA that is a clinically widely used assay for detecting biomarkers. The researchers that carried out a clinical study on the measurement of serum among patients with oral cancer reported that ELISA showed sensitivity to CD44 protein; however, for more comprehensive sample size and a more significant number of patients, experiments should be conducted on a better assay [7]. A study on gastric cancer samples concluded that ELISA is predisposed to cross-contamination and presented lower sensitivity than multiplexing electrochemical detection assay [8].

1.2 Aims and Objectives

The main goal of this study is to construct an accurate biosensing platform that detects cancer biomarker CD44 in a dynamic setup using a fiber optic sensor fabricated in the laboratory with the advantages of being low-cost and fast to implement. The following objectives are pursued in this regard:

I. Fabrication of fiber optic biosensor using standard single-mode fibers
II. Calibration of fiber optic biosensor for further selection for functionalization
III. Fiber optic surface functionalization
IV. Dynamic measurement of CD44
    V.I. *In-vitro* platform
V. Fiber optic surface morphology study

Chapter 2 – Literature Review

2.1 Introduction

Despite tremendous medical advancements, cancer still poses a serious problem on a global scale. According to the Global Cancer statistics 2020 cancer report, the number of cancer cases and cancer-related fatalities worldwide is steadily rising each year, and in 2040, it is predicted that there will be 28.4 million cases of cancer [9]. In Kazakhstan, cancer is the second leading cause of death after cardiovascular diseases. Due to a lack of medical equipment for diagnosis and treatment and a shortage of personnel, oncological care is not given uniformly in all regions of Kazakhstan [10]. Cancer metastasis, which is strongly correlated with the presence of circulating tumour cells in human blood, is responsible for more than 90% of cancer-related death [11]. According to the World Health Organization, an early cancer diagnosis is crucial since many cancer cases can be successfully treated with early detection and efficient therapy. Early diagnosis and a screening program are the two methods of early detection of cancer recommended by WHO. A cancer diagnosis is based on the patient's symptoms, although symptoms typically do not present until the disease has progressed considerably[4].

Metastases are a leading cause of cancer-related mortality and morbidity. During metastasis, cancer cells travel from the initial lesion to secondary organs, where they may lie dormant for a considerable amount of time before re-emerging. The development of metastases is still the sign that patients with tumours and clinicians worry about the most. Even while advances have been achieved in earlier detection and more targeted treatment, most cancer patients' deaths are due to metastases in other parts of the body [12].

2.2 Importance of CD44 as a cancer biomarker

Today, there is a significant amount of interest in the identification of cancer-specific biomarkers for the early-stage diagnosis of a wide variety of cancers and the clinical management of these tumors. Yan et al. state that "biomarker" refers to a quantifiable biological activity utilized as a predictor of disease risk or health status [13] . CD44 is one of the few proteins known to play a substantial role in this process [4].

The transmembrane glycoprotein CD44 plays an important part in cell proliferation, motility, adhesion, and signal transduction. CD44 has a molecular weight of 85-200KDa and is expressed by a wide variety of cell types [2]. It was previously believed that CD44's only function was as a transmembrane adhesion molecule involved in the metabolism of its primary ligand, hyaluronic acid. Over the past 20 years of research, CD44's many roles have been elucidated. These include its ability to mediate inflammatory cell activity and tumour growth and metastasis [14]. CD44 is a protein expressed by a single gene found on the short arm of chromosome 11 in human [15]. However, due to alternative RNA splicing, different isoforms of CD44, like standard and variant are produced. There are a total of 20 exons contained inside the CD44 gene, and 12 of them are expressed by the "standard form," which is the most prevalent form of CD44 [14]. Cleavage of transmembrane CD44 is done on both sides by proteases. When the extracellular domain of CD44 is cleaved, it leads to shedding, thus increasing soluble CD44 in circulation [16]. While shedded intracellular domain of CD44 in the cytosol enters the nucleus and controls gene transcription for the synthesis of new CD44, thus promoting metastasis [17]. In addition to being a key surface biomarker in the proliferation of cancer stem cells that lead to metastasis, CD44 also encourages the epithelial-mesenchymal transition by activating a number of signalling pathways, which causes the cell to invade and spread the malignancy[5].

Numerous clinical studies reported that the elevated level of CD44 protein was associated with cancer progression. Increases in soluble CD44 levels in serum were initially reported by Guo et al. (1994) in patients with colon and stomach cancer. These authors hypothesized that this molecule could be used as a good marker in patient monitoring because the levels of serum CD44s were closely associated with the burden of the tumour (Ziemet et al., 1997). Several studies have pointed to CD44 as a possible biomarker of the progression of cancer; when patients with ovarian cancer were compared to healthy controls, researchers found that patients with ovarian cancer displayed greater sCD44std levels [18]. Furthermore, it was shown that modest quantities of soluble CD44 may be present in the blood of healthy people and the joints of those with rheumatoid arthritis. In the clinical study, the serum of healthy individuals contained around 2.7 + 1.1 nM of soluble CD44, advanced gastric and colon cancer patients were shown to have significant levels of soluble CD44 in their blood, measuring 24.2+9.8nM and 30.8+11nM, respectively. Cancer metastasis and the amount of soluble CD44 in the serum were significantly correlated. 16 of the 17 gastric cancer patients with metastatic disease exhibited elevated CD44 serum concentrations. In 14 of the 15 metastatic colon cancer patients analyzed, there was a substantial rise in CD44 concentrations [19]. Correlation between the soluble form of CD44 and tumor burden was also observed in breast cancer, head and neck squamous cell carcinoma, cervical and gastric cancer [4]. As a surface biomarker, CD44 encourages the growth of cancer stem cells, thus leading to metastasis, moreover, it stimulates the epithelial-mesenchymal transition, which causes the cell to penetrate and disseminate cancer by activating a number of signaling pathways [5].

Transmembrane glycoprotein CD44's expression was observed on both embryonic stem cells and mature cells, like leukocytes, fibroblasts, epithelial, mesodermal, keratinocytes, endothelial cells, and neuroectodermal cells [20]. Association of CD44 to metastasis and

tumorogenesis can be addressed to its high expression in cancer stem cells (CSC) and different cancer cell types like epithelial ovarian cancer cell [21], breast cancer [22], head and neck squamous carcinoma [23], colorectal cancer [24], oral squamous cell carcinoma [7]. CD44 is a considered as a key diagnostic biomarker that identifies some types of cancer via examination. The role of CD44 in tumor initiation and development has been proven to be associated with cancer stem cells (CSC) and the epithelial-mesenchymal transition program [3]. According to studies, CSCs are resistant to chemotherapy and radiotherapy due to their role in the initiation and persistence of tumor growth [23]. Several studies have shown an association between CD44 and tumor growth and metastasis; in head and neck squamous cell carcinomas, CD44 is also implicated as a CSC marker. Because there are no outward signs of mouth cancer, earlier detection is challenging. This lowers the detection rate, hence it's critical to develop a reliable detection technique. OSCC that has progressed to the lymph nodes at an advanced stage has a bad prognosis, but only approximately half of cases are found before they have reached the neck lymph nodes [25].

2.3 CD44 detection methods

In clinical studies, the measurement of CD44 is mainly done on an established and often-used test ELISA. Researchers conducted a clinical study on the measurement of serum among patients with oral squamous cell carcinoma reported that ELISA showed sensitivity to CD44 protein; however, experiments should be carried out on a better assay for a larger sample size and a more significant number of patient [7]. Another clinical trial using samples from patients with stomach cancer concluded that multiplexed electrochemical detection assays are more sensitive and resistant to cross-contamination than ELISA [8]. These investigations came to the conclusion

that a reliable, user-friendly CD44 biomarker detection approach is required in order to increase the success of cancer therapy via early cancer detection.

To identify CD44 protein, many platforms and sensors have been created, such as optical fiber biosensors, photoelectrochemical biosensors, and electrochemical impedance spectroscopy. These platforms might serve as a good alternative to the time- and money-consuming classical ELISA. The present commercially available methods for detecting CD44 protein have limitations in terms of cost and usability, including the need for labeling, extended detection times, and inapplicability for *in vivo* use due to electromagnetic interference. Because of recent advancements in the field of biosensors, using biomarkers to detect cancer is becoming more popular. Some ongoing projects for developing electrochemical biosensors, photoelectrochemical (PEC) technologies with antifouling interface biosensors, and fluorescence assays are focused on the detection of CD44 biomarker. The study for developing biosensors proposed by Fan et al. (2019) includes the features of two different photo- and electrochemical detection methods of CD44 biomarkers. Hyaluronic acid and polyethylene glycol were co-immobilized for the target protein CD44, thus achieving synergistic antifouling activity. It is reported that the proposed method is distinguished by the simplicity of its development and usage compared to the traditional ELISA, as well as the equally important fact that it is antibody-free and has high sensitivity [6]. The authors also claim that the biosensor has good antifouling properties by testing it in IgG and PSA as biofouling agents; however, the drawback of this biosensor is that it can not be used for in vivo studies [6].

At least two clinical trials are ongoing with OncAlert, and this method is designed for CD44 biomarker detection in the saliva of patients. A commercially available rapid test called OncAlert for early identification of oral and oropharyngeal cancer before lesions are apparent. The

OncAlert rapid test provides a qualitative evaluation at the point of care by disclosing levels of the oral cancer biomarker CD44. This technique is fast, requiring around 15 minutes, and a non-invasive and simple platform for detecting CD44; however, it only provides qualitative data [26].

Biosensor based on an optical fiber sensor was developed for the detection of CD44 protein. Light is transmitted via optical fibers by total internal reflection. The core and cladding of an optical fiber have different refractive indexes, and as light enters the core, some of it passes through a reflecting medium that can distinguish between different refractive indexes [27]. Using a standard single-mode fiber which is telecommunication grade fiber and a CO_2 splicing machine, an optical fiber biosensor could be fabricated in about a couple of minutes, and then it is proceeded for further functionalization after confirming its sensitivity to refractive index change [28]. Because of its advantages like, compactness, resistance to electromagnetic interference, low cost, chemical inertness, low limit of detection, fast fabrication and availability for *in vivo* applications, optical fiber biosensor could be a valuable biosensing platform for the detection of biomarkers [27]. Furthermore, it can be used for multiplexing purposes and target independent, which means that it can detect multiple targets and different biomarkers [29]. Multiple analytes can be determined or monitored in a single location by using a single central unit because it is capable of directing light of different wavelengths at the same time [27]. Optical fiber biosensor have been used as a sensor platform for many different applications, including sucrose, glucose, heavy metals, DNA, cancer biomarkers.

CD44 is a cancer-related biomarker that plays a vital role in the invasion and spread of cancer; hence, the detection and quantification of CD44 can offer essential information that is relevant for clinical cancer diagnosis. In this perspective, the development of CD44 detection platforms is given priority by biosensors with sensitive and selective features. The purpose of this

study is to build an accurate biosensing platform that detects the cancer biomarker CD44 in a dynamic setup in the direction of clinical application using a laboratory-fabricated fiber optic ball resonator.

Chapter 3 – Experimental Components

Chapter 3 presents detailed fabrication and functionalization processes of ball resonators with further CD44 cancer biomarker detection measurements and surface morphology studies. In this study, to develop an optical fiber biosensor for the detection of CD44 protein, single-mode (SMF-28) fiber was spliced, and a sphere was fabricated on the tip of single-mode fiber using a Fujikura LZM-100 CO_2 splicing machine. After fabrication, ball resonators were selected based on the results of calibration. Measurement of fiber optic biosensors with different concentrations of sucrose solution was done to determine reflectivity and sensitivity to refractive index on static and dynamic setups. Then calibration data were analyzed on MatLab software to select fiber optic biosensors for further steps based on the sensitivity to the refractive index change. The next step was a surface functionalization of the optical fiber biosensor, which was performed in multiple steps to attach ligands for CD44 protein detection. When the functionalized biosensor was ready, the CD44 detection measurements were done on a dynamic setup. Furthermore, the surface morphology of the biosensor was studied on atomic force microscopy. **Figure 1** shows the steps of the experimental part of the study.

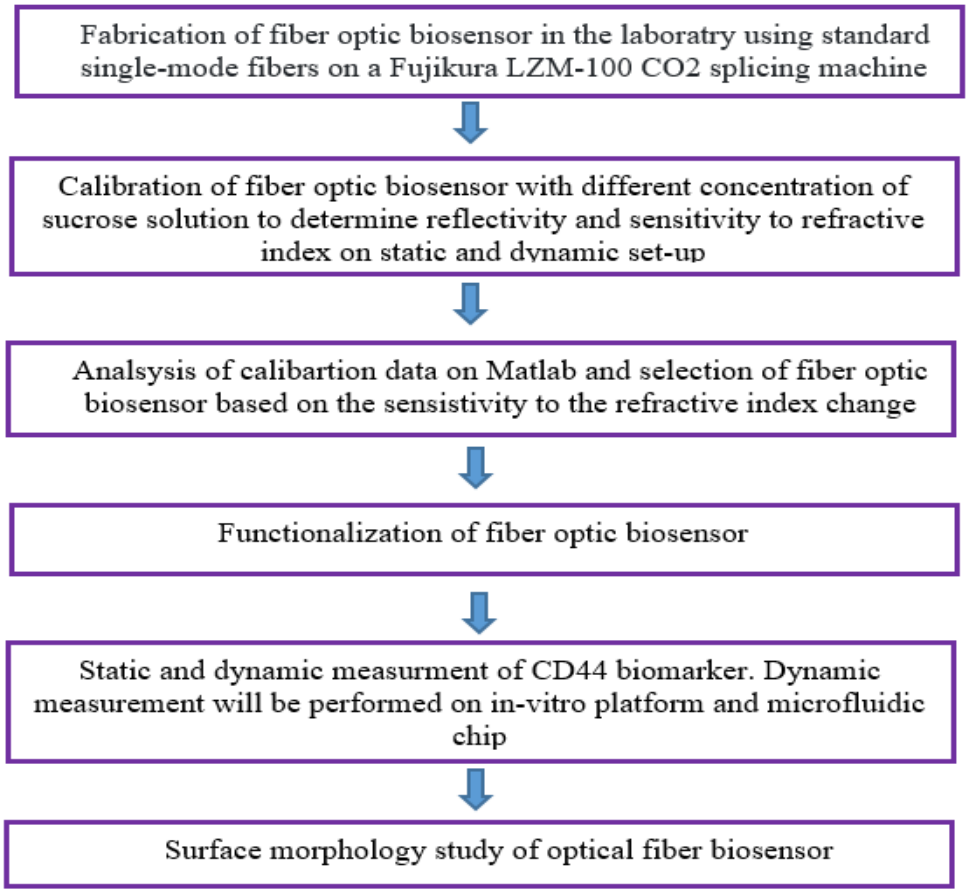

Figure 1. The flow diagram represents the methodology of the study.

3.1 Optical fiber ball resonator fabrication

Optical fiber ball resonator was fabricated from single mode fiber-28, SMF-28, using the CO_2 splicing machine Fujikura LZM-100. SMF-28 is mainly made of silica with core and cladding diameters of 8.2 μm and 125μm, respectively. Two single-mode fibers were polished from cladding 2 cm from the end and placed into the Fujikura 100-LZM for further ball resonator fabrication, as shown in **Figure 2c**. The device produces a spherical tip by aligning, splicing, heating, and pulling procedures with two single-mode optical fibers. A spherical ball resonator was produced at the endpoint of the optical fiber with a diameter of around 500μm. Before

fabrication of the ball resonator with Fujikura LZM-100, the machine must warm up for a couple of minutes. After warming up, Star Lab software should be opened from the computer to set parameters for fabricating the ball resonator. After motor adjustment, equipment must be calibrated with non-cleaved but stripped SMF-28 to get calibration data.

Figure 2. Fujikura LZM-100 machine (A) with interaction window (B) and single mode fiber placing area (C).

After equipment calibration, the splicing mode and lens for the ball resonator were chosen. It is necessary to switch from a power calibration regime to a special splicing regime; in this case, it is Mode 43 in order to fabricate a ball resonator. At this point, Fiber Processing Software, FPS

was opened from the computer, where customization of the ball resonator dimensions was adjusted. Several physical characteristics and settings must be set; including the ball diameter, diameter adjustment, distance from the splice, and splice offset; **Figure 3** shows settings adjustment for the fabrication of the ball resonator using FPS. In order to produce a spherical ball lens, optical fiber is heated and rotated inside the Fujikura LZM-100. As part of the configuration process, absolute power and rotation speed are configured. The feeding speed is typically adjusted between 0.025 and 0.1 mm/s; faster speeds may result in defective ball resonators. The fabrication of the sensor was initiated. Relative power, break add power, rotation and movement, and diameter values were chosen for the optimal size of the ball resonator. It is necessary to set up all the characteristics of the ball resonator in the software by clicking the initiate button.

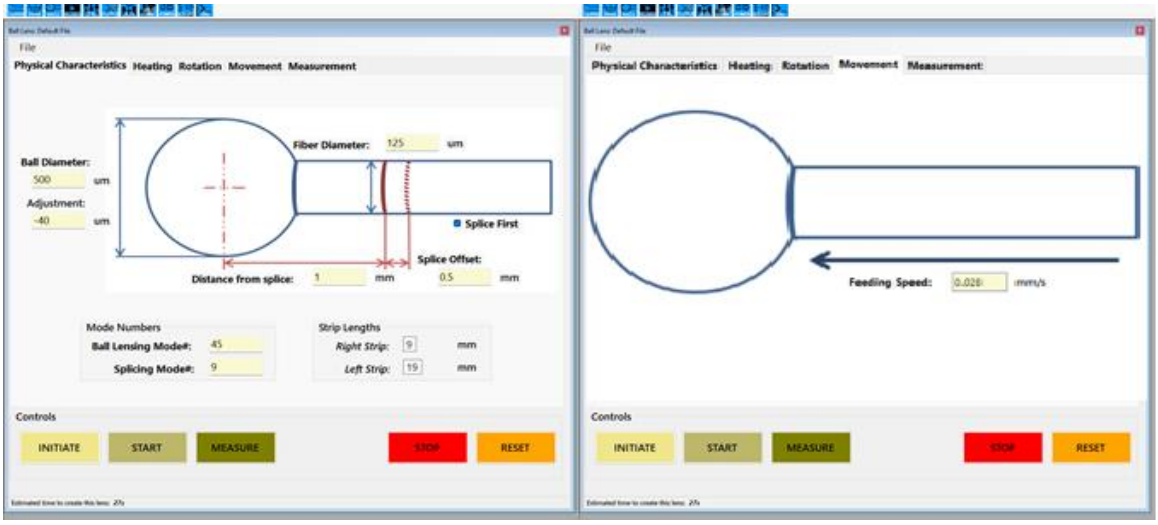

Figure 3. Settings adjustment for fabrication of the ball resonator using FPS.

Upon successfully configuring the Fujikura LZM-100 device, two optical fibers without coating on one end are placed in adjacent V-grooves with their uncoated ends almost touching each other, right above the CO_2 laser. To prepare these fibers, 10 cm in length bare SMF-28 were taken; these 2 fibers must be stripped with a fiber stripper to remove the coating, and a diamond

cleaver must then be used to cut the stripped end, leaving a perfect splice cut. When everything was set, stripped and cleaved fibers were placed in Fujikura LZM-100. The lid should be closed to prevent laser leaks and potential eye or skin damage, then set button was pressed. After the optical fibers were spliced, they were offset and then rotated with heating, expanding and gradually becoming spheres. When the ball resonator was ready on the screen of fabricating machine Fujikura 100-LZM the image appeared as in **Figure 4**.

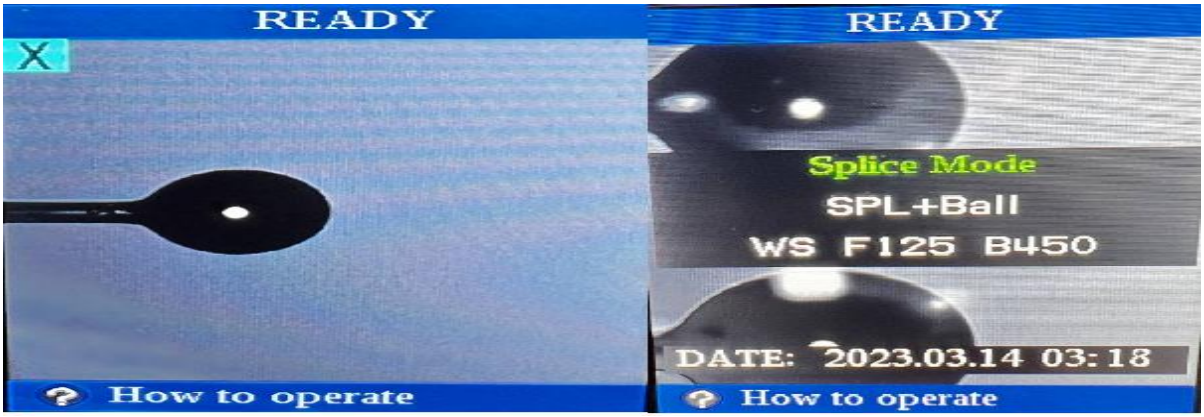

Figure 4. The image appeared on the interaction window of Fujikura LZM-100 when the ball resonator was fabricated.

The ready ball resonator must be measured, and a report is created with ball resonator diameters and characteristics, as shown in **Figure 5.** An individual sensor takes approximately 1-2 minutes inside the Fujikura LZM-100, while the whole preparation process lasts about 5 minutes. The actual image of the fabricated optical fiber ball resonator with a diameter of 492-485 μm is shown in **Figure 6.**

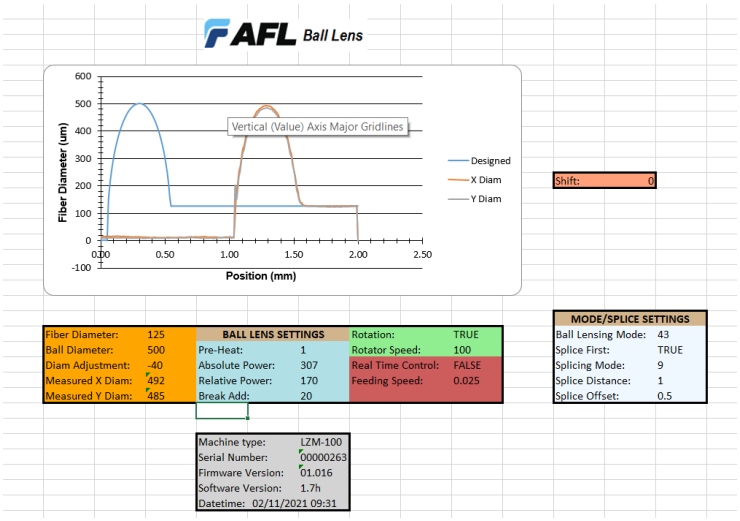

Figure 5. Created report by FPS when ball resonator was successfully fabricated.

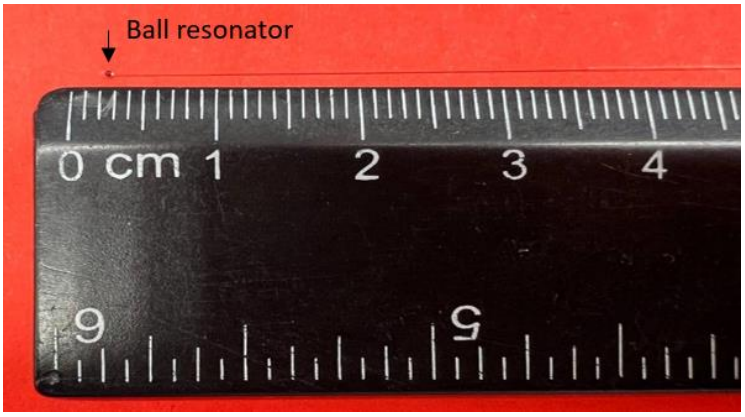

Figure 6. Fabricated ball resonator with a diameter of 492-485 µm.

3.2 Optical fiber ball resonator calibration

Readily fabricated ball resonators with specified diameters proceeds for further selection based on reflectivity and sensitivity to refractive index (RI). This measurement was performed using optical backscatter reflectometer (OBR), LUNA OBR 4600 equipment with the computer for data analysis. The fabricated ball resonator was stripped and spliced using the splicing machine,

Figure 7, to connect the pigtail connector to the fabricated ball resonator. After splicing the ball resonator, it was connected to the optical backscatter reflectometer.

Figure 8. Special diamond cleaver (A) and Fujikura 36S Splicing machine (B). Splicing process of fabricated ball resonator to the pigtail (C).

Before the measurement, the optical backscatter reflectometer must undergo calibration with a reference reflector. Among the fabricated optical fiber ball resonators, high reflectivity values and high sensitivity to refractive index (RI) change were considered prior to functionalization. Different sucrose solutions with known RI values were used during the calibration process. 10% sucrose solution with a volume of 6ml is measured first, followed by 400 µl of 40% sucrose solution at each step. **Table 1** represents the sucrose solutions with known RI values. Calibration with different sucrose solutions was done in static and dynamic conditions. The same concentrations were used in dynamic sucrose solution calibration, while the volume was different. 30 ml of 10% sucrose was taken into the syringe for the first RI calibration data, followed by adding to 30 ml of 10% sucrose solution, 2 ml, 4 ml, 6 ml, and 8 ml of 40% of sucrose solution for dynamic RI measurements. The same sensor was calibrated on static and dynamic conditions to compare the sensitivity.

Table 1. H_2O and sucrose solution concentration with known RI value.

	Sucrose concentration	**RI value**
H_2O	0%	1.33304
Sucrose 10%	10%	1.34761
Sucrose 10% + 400 µm of 40% sucrose	10.97%	1.34974
Sucrose 10% + 800 µm of 40% sucrose	11.87%	1.35216
Sucrose 10% + 1200 µm of 40% sucrose	12.73%	1.35457
Sucrose 10% + 1600 µm of 40% sucrose	13.53%	1.35696

3.3 Optical fiber ball resonator surface functionalization

After the sensor calibration, ball resonators were selected for further functionalization based on high reflectivity and sensitivity to RI change. Using MatLab software, ball resonators sensitivity and coefficient of determination, R^2 were calculated and graphs were produced. Functionalization of the optical fiber sensor begins with pre-treatment using the Piranha solution. Piranha solution constituted sulfuric acid and hydrogen peroxide. 3 ml of H_2O_2 was to the 12 ml of H_2SO_4, composing 1:4 ratio, into this prepared Piranha solution. Ball resonators attached to the glass rods were immersed for 15 minutes. After 15 minutes, ball resonators were washed thoroughly with deionized H_2O several times and dried with nitrogen (N_2) gas. After the Piranha cleaning from organic residuals ball resonators proceeded for treatment with 1% (3-aminopropyl)trimethoxysilane (APTMS) solution for 20 minutes, which was prepared by taking 14.85 ml of methanol and 150 µl of APTMS. Upon treatment with APTMS, ball resonators were rinsed with methanol and placed into the oven for 1 hour at 110°C. Ball resonators were washed

with DI water after heat treatment, then proceeded for 25% glutaraldehyde solution incubation for 1 hour. 500 µl of phosphate buffer solution (PBS) was added into 500 µl of 50% glutaraldehyde after 1-hour ball resonators were washed with PBS. The next functionalization step was antibody immobilization to the surface of the ball resonator; for this 4 µg/ml concentration of CD44 monoclonal antibody was used. From the stock 1 mg/ml CD44 antibody, 4 µl was added into 996µl of PBS, then into the prepared 4µg/ml CD44 antibody solution ball resonators were incubated for 1 hour under continuous shaking. After attachment of the CD44 antibody, ball resonators were incubated into the 10% poly(ethylene glycol) methyl ether amine (m-PEG amine) solution prepared by weighting 0.05 g of m-PEGamine and dissolving it in the 500 µl of PBS. Ball resonators were incubated in the blocking agent for 30 minutes, followed by washing with PBS. Functionalized and ready-to-use ball resonators were stored in the PBS solution at 5 °C; images from all steps are shown in **Figure 8.**

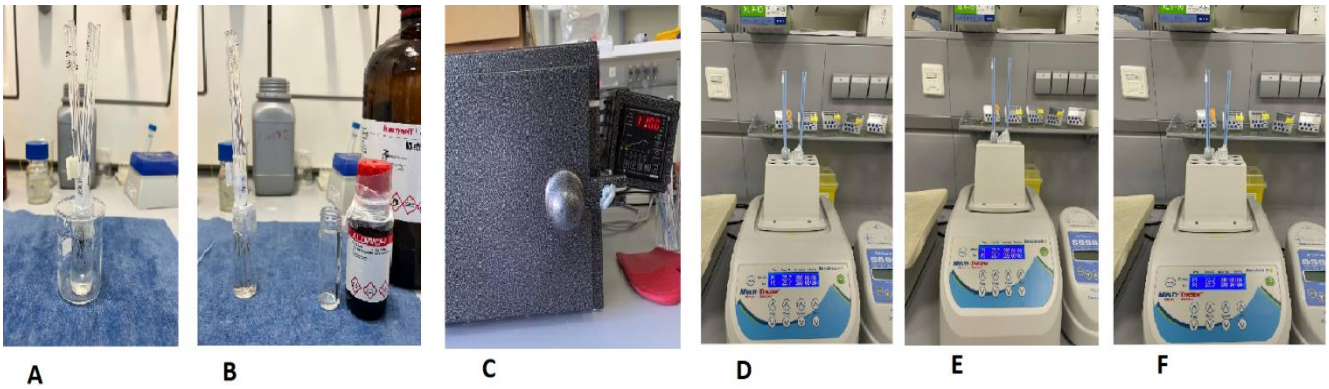

Figure 8. Optical fiber ball resonator functionalization process for the detection of CD44. Pre-treatment (A) Silanization (B) Heat-treatment (C) Cross-linking with GA 25% (D) Antibody immobilization (E) Blocking (F)

3.5 Dynamic protein measurement

A dynamic protein measurement system was developed to simulate dynamic blood flow through veins by measuring CD44 protein *in vitro*. A syringe pump (Legato 100, KD Scientific)

can generate different flow rates; during protein measurement, the pump was set to 20 ml/min to mimic blood flow in the vein. CD44 protein solution at concentrations of 7.1aM, 9.3 fM, 12.9 pM, and 16.7 nM was pumped through a 1 mm diameter tube at a 20 ml/min flow rate. Before the protein measurement experiment, the tubing used for protein measurement was blocked with 1 % bovine serum albumin (BSA) for 1 hour at a flow rate of 1 ml/min. 1% of BSA was prepared by weighing 0.6 g of BSA and dissolving it in PBS. CD44 protein was measured in diluted calf serum (1:10), and 33 ml of serum was added to the 297 ml of PBS. From stock 17390 nM CD44 protein, 57.7 µl was added into the 60054 µm diluted calf serum, thus making 16.7nM of CD44 protein. Averaged 45.2 µl were transferred to the next bottle with 60054 µl of diluted calf serum, resulting at 12.9 pM. Serial dilution was done with 24X, and CD44 protein with concentrations of 16.7 nM, 12.9 pM, 9.3 fM, 7.1 aM and a total volume of around 60 ml each were prepared for a dynamic measurement; a schematic picture is shown in **Figure 9.** The specificity tests were done with control protein Thrombin and gamma globulin.

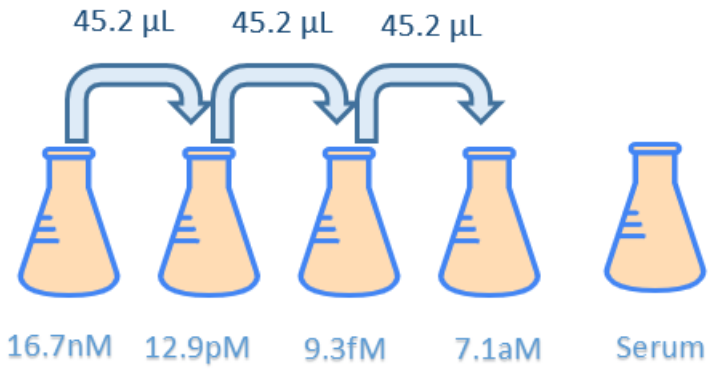

Figure 9. CD44 concentration preparation for *in vitro* studies. Each

Catheter 20 gauge, G, made of polyurethane, PUR, was sealed on the tip, and the ball resonator area was removed to provide mechanical protection; a schematic image of the catheter with and without a ball resonator is demonstrated in **Figure 10.** The size of the catheter in length is 32mm, and the internal diameter is around 1.1mm. The tubing was punctured with a tricut bevel needle allowing the catheter to stay inside the tubing. A small hole was made in the taper luer lock connection for the optical fiber biosensor insertion. Once the ball resonator was inside the catheter, the hole is sealed with clay, and the ball resonator was connected to the LUNA OBR 4600. Each concentration measurement lasted approximately 3 minutes, and every measurement was around 10 seconds, producing around 18 measurements.

Figure 10. Modified catheter for CD44 detection without and with ball resonator inside.

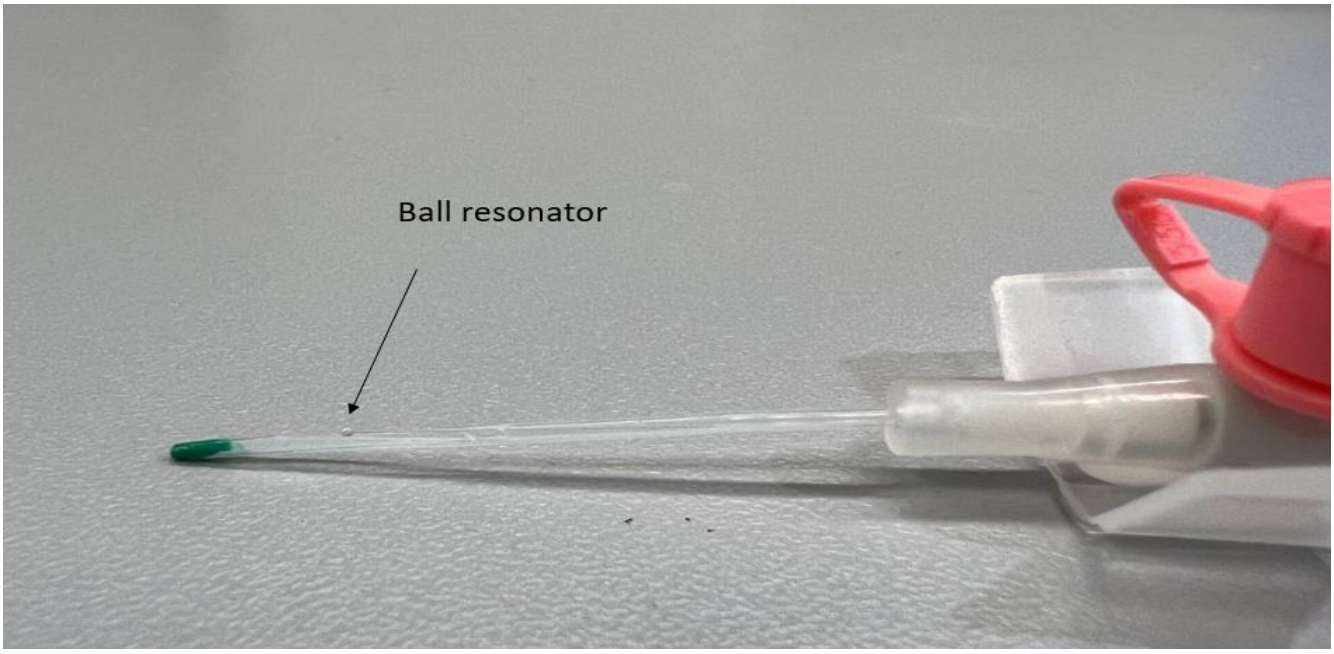

Figure 10. The actual image of optical fiber ball resonator inside 20G catheter.

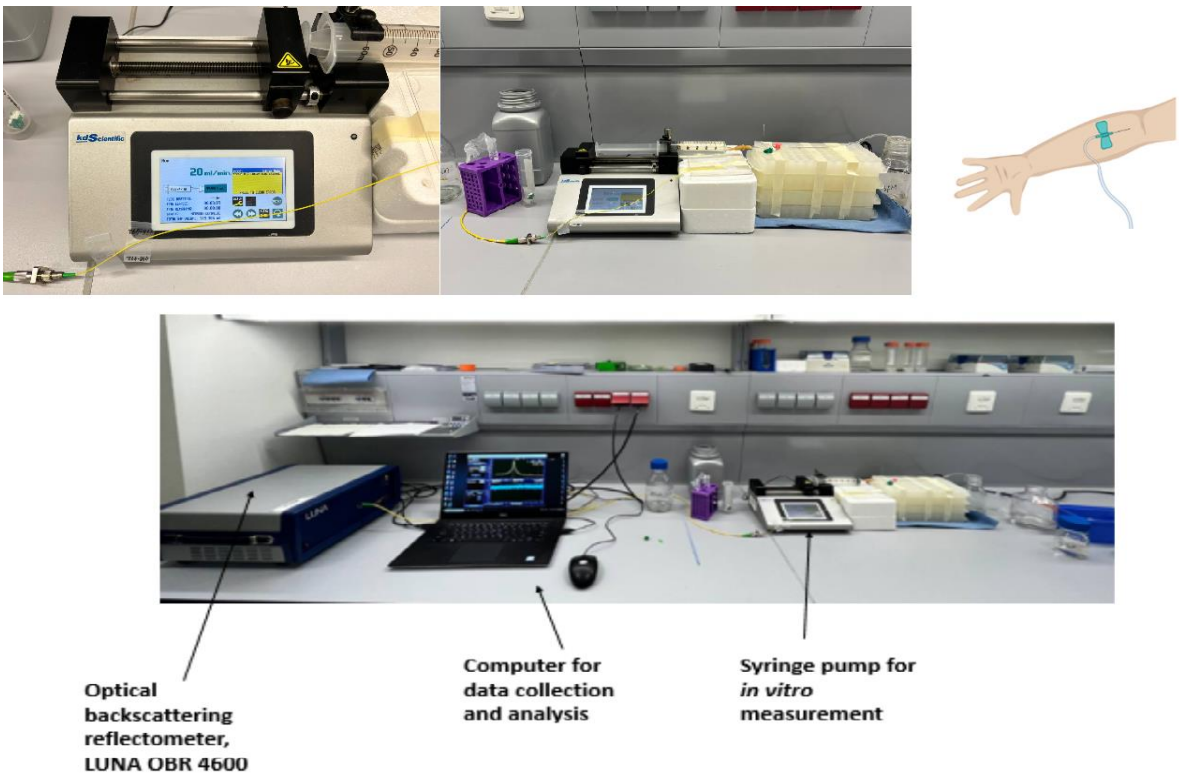

Figure 11. CD44 protein dynamic measurement setup.

3.6 The pressure characterization.

The pressure characterization of an optical fiber ball resonator was done to ensure the measured signal is not because of pressure. An optical fiber ball resonator was inserted into the burette from the tip and sealed with clay to protect it from leaking. Burette was fixed on the stand and optical fiber ball resonator with a 499-494 μm diameter connected to the optical backscattering reflectometer. From the top of the burette, DI water was poured. Measurements were taken at 16 cm, 26 cm, 36cm, 46cm, 56cm, and 66 cm. The pressure measurement setup is shown in **Figure 12.**

Figure 12. Pressure characterization of a ball resonator.

3.7 Surface morphology study

Bruker Nanowizard 4XP AFM coupled with an inverted ZEISS Axio Observer 7 microscope was used to study the morphology of the sensor on each step of functionalization. For this, 3 ball resonator sensors were taken after each step of surface modification and kept in PBS before being analyzed. A cantilever (Bruker AFM Respa20 probe) with a characteristic resonant frequency of 13 to 27 kHz and a force constant of 0.45 to 1.8 N m^{-1}. All measurements were performed in liquid (PBS) using a contact mode force mapping regime. Triplicate scans of each sample were taken across a scan region ($1 \times 1\ \mu m^2$), and root mean square Roughness (RMS) was then calculated. SEM Crossbeam 540 instrument was utilized to analyse optical fiber ball resonator surface morphology.

Chapter 4 – Results and Discussion

The purpose of this work was to assess the feasibility of developing an optical fiber biosensor that can identify the CD44 protein under dynamic conditions. Using a CO_2 splicing machine, a ball resonator was made on the tip of a single-mode telecommunication fiber. During the optical fiber ball resonator fabrication process with the Fujikura LZM-100 device, ball resonators with different diameters were manufactured, as listed in **Table 2.** The last step of the study involved data processing; MatLab software was used for this. MatLab code was created to extract data from the "txt" files of the lower graphs and display it in MatLab plots. A 2D profile of the fabricated ball resonator was done using data from the Fujikura report after ball resonator fabrication, shown in **Figure 13.** Sensitivity and R^2 values were calculated using MatLab software from the data taken from sucrose calibration. On LUNA OBR software, OBR files were loaded and assessed for the trend, shown in **Figure 14.** These analyses were done to select optical fiber ball resonators with high sensitivity and R^2, a coefficient of determination over 0.95.

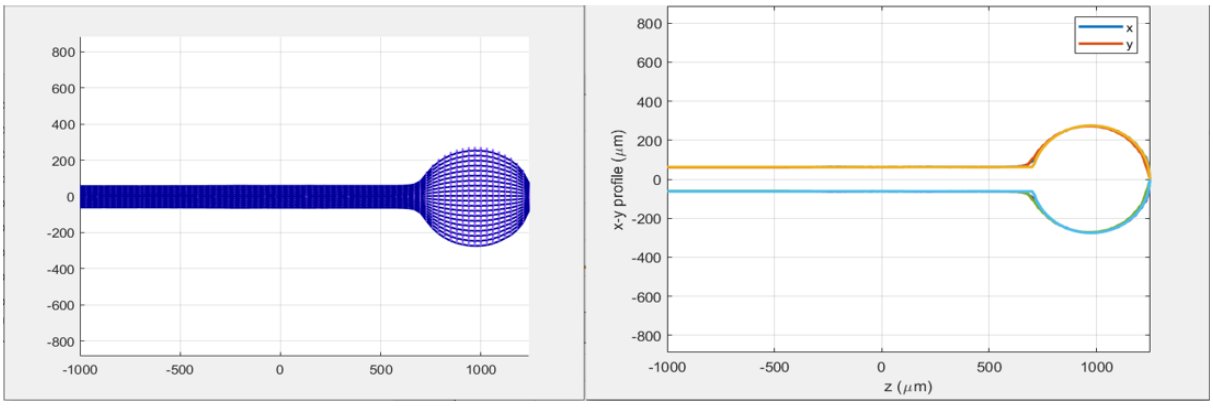

Figure 13. The geometrical 2D profile of a ball resonator 492-485 μm fabricated by Fujikura LZM-100.

Table 2. Optical fiber ball resonator data.

	Diameter (µm)	Reflection dB/mm	Sensitivity (dB/RIU)	R^2	At the wavelength (nm)	Purpose
1	489-492	air:35 water:47	**-96**	**1,00**	1 565,42	Gamma globulin detection
2	491-485	air:35 water:48	**-90**	**0.96**	1 552,75	CD44 detection
3	492-485	air:37 water:47	**-98**	**0,95**	1 573,42	CD44 detection
4	496-491	air:35 water:45	**-83**	**0,99**	1 552,98	CD44 detection
5	497-492	air:35 water:50	**-98**	**0,95**	1 571,60	CD44 detection
6	497-491	air:36 water:48	**-74**	**0,99**	1 553,14	Pressure measurement
7	499-494	air:36 water:48	**-85**	**0,97**	1 552,85	CD44 detection
8	521-515	air:37 water:49	**-128,37**	**0,98**	1 552,55	CD44 detection
9	533-527	air:36 water:46	**-105**	**0,97**	1 580,55	CD44 detection
10	485-491	air:37 water:50	**-83**	**0,98**	1 552,88	Thrombin detection
11	518-510	air:44 water:54	**-105**	**0,95**	1 565,42	Thrombin detection
12	499-494 (1)	air:36 water:48	**-84**	**0,97**	1 570,99	Pressure measurement

Dynamic sucrose calibration was also performed, and there was almost no difference between values, **Table 3** compares values of static and dynamic sucrose calibration. During *in vitro* measurements, until the optimization of dynamic setup, some bubbles were formed because there was not proper sealing from the catheter side, and the air was entering the tubing.

Table 3. Comparison of static and dynamic sucrose calibration data.

Sensor size	**Static Reflection dB/mm**	**Static MatLab analysis**	**Dynamic Reflection dB/mm**	**Dynamic MatLab analysis**
527-520µm	air-33 water-53	R^2-**0.99** Sensitivity-83 dB/RIU	air-33 water-50	R^2-**0.95** Sensitivity-**83 dB/RIU**
514-505 µm	air-35 water-47	R^2-**0.99** Sensitivity-86 dB/RIU	air-33 water-45	R^2-**0.95** Sensitivity-**85 dB/RIU**

Sensors with the diameter size of 527-520µm and 514 -505 µm were calibrated in static and dynamic measurement, and the following results were obtained after analyzing by MatLab software. R^2, the coefficient of determination, decreased probably due to the 20 ml/minute flow rate mimicking blood flow, but the sensitivity of the ball resonator remained the same. According to the calibration results analyzed on a MatLab software, a ball resonator with a diameter of 528-522 µm had a sensitivity 77 dB/RIU and R^2 was 1.0. **Figure 14** represents sucrose calibration results of a ball resonator with a diameter of 528-522 µm. A nice trend can be seen, blue line starts with the lowest sucrose concentration 10%, red line is the second sucrose concentration 10.97%, green line is the third 11.87% sucrose concentration, yellow line is the fourth 12.73% sucrose concentration and the pink for the last 13.53% sucrose concentration measured.

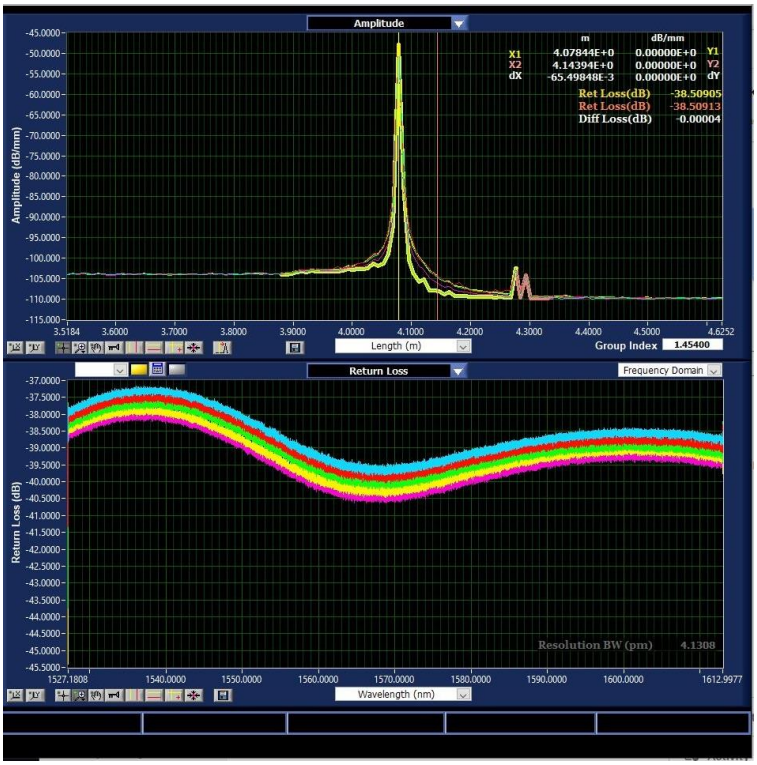

Figure 14. Sucrose calibration results of a ball resonator with a diameter of 528-522 µm.

Figure 15 compares different sucrose calibration results. **Figure 15A** shows the results of the ball resonator with a diameter of 521-516 µm and a sensitivity of -149 dB/RIU, and R^2 was 0.73, while the second sensor on **Figure 15B,** a sensor 520-514 µm showed a sensitivity -83 dB/RIU and R^2 0.94; **Figure 15C** a sensor 528-522 µm sensor presented a sensitivity -77, and R^2 1.00 and on Figure **15D** 539-534 µm sensor had a sensitivity -88 dB/RIU and R^2 was 0.99**.** A preliminary analysis of the sucrose calibration results of the ball resonator could be done before analyzing it on MatLab software.

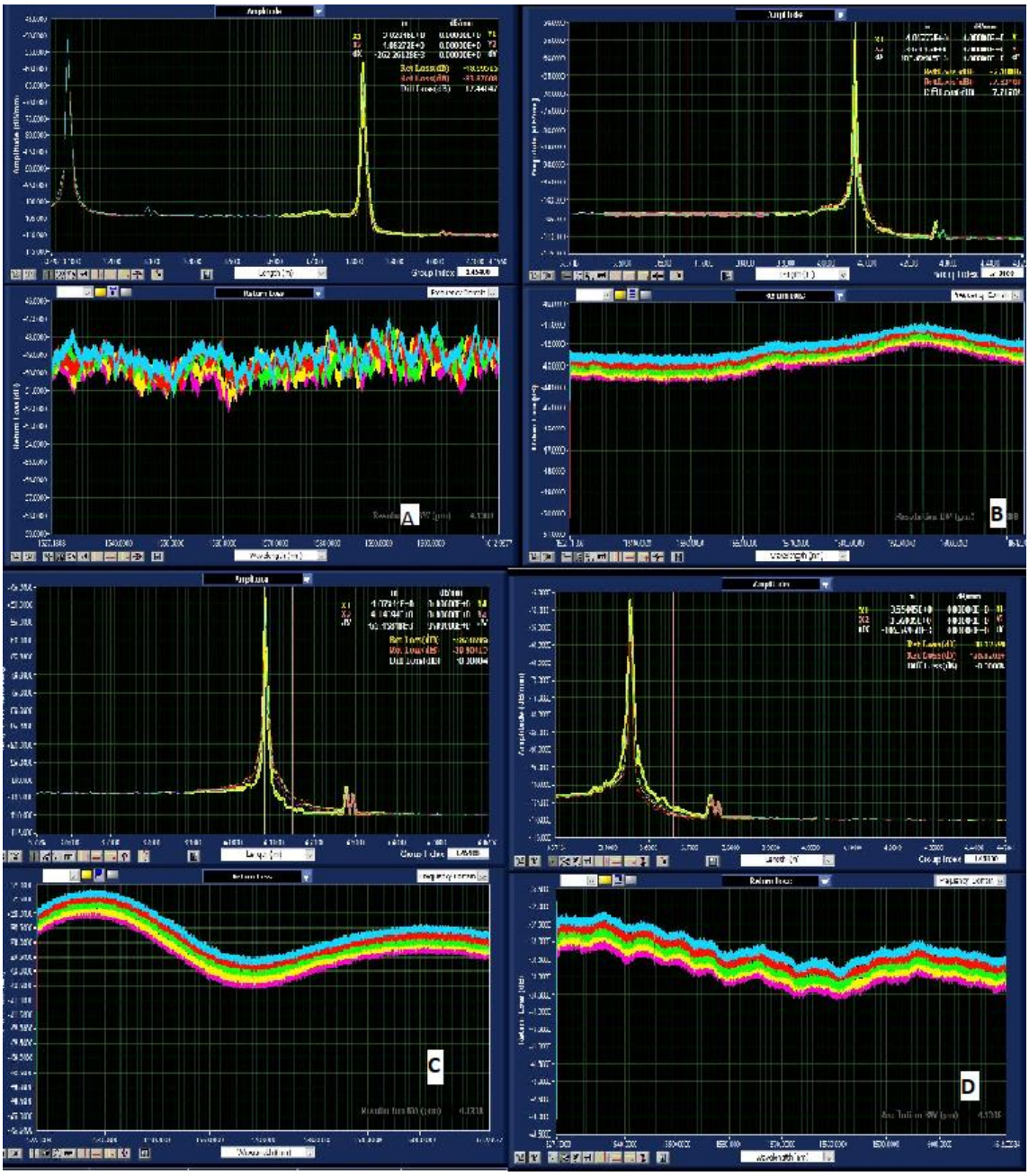

Figure 15. Comparison of calibration results of optical fiber ball resonators with different diameters (A) 521-516 µm and sensitivity -149 dB/RIU and R^2 was 0.73 (B) 520-514 µm and sensitivity -82 dB/RIU and R^2 was 0.99 (C) 528-522 µm and sensitivity -77 dB/RIU and R2 was 1 (D) 539-534 µm and sensitivity -88 dB/RIU and R^2 was 0.99.

Calibration results showed that the optical fiber biosensor is sensitive to changes in surrounding RI. Calibration results are shown in **Figure 16** for 2 sensors. Sensors with high sensitivity and R^2 over 0.95 were chosen for protein functionalization.

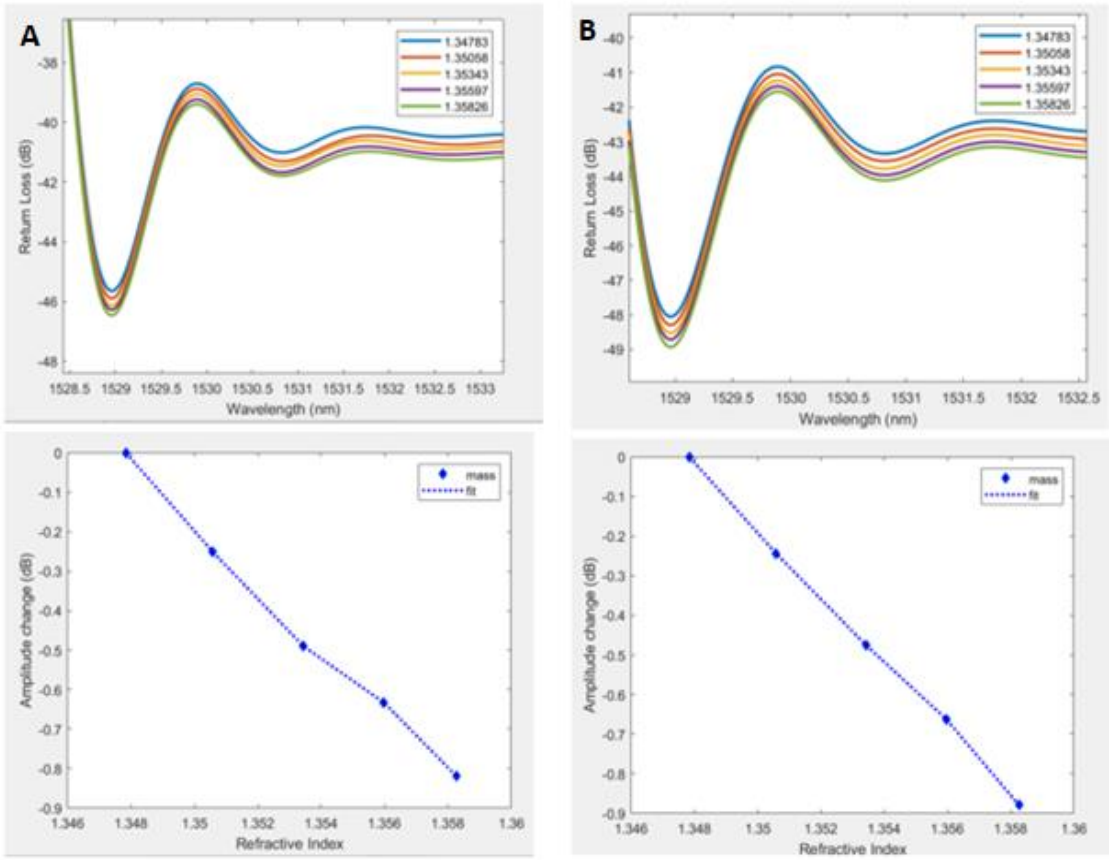

Figure 16. Sucrose calibration graphs produced after analyzing by MatLab software (A) 491-485 µm (B) 520-514 µm.

Dynamic CD44 detection was performed to determine the optical fiber ball resonators' potential to capture CD44 protein. CD44 protein is not a very common circulating cancer protein in the blood; therefore, analyzing a substantial blood volume will allow an accurate diagnosis. In order to accomplish this, an intravenous catheter conjugated with an optical fiber ball resonator was pierced into the tubing. Inside the tubing, there was protein in diluted calf serum with a flow

rate of 20 ml/min mimicking a blood flow. During the CD44 detection assay, a concentration-dependent increase in signal was observed. In our previous study, we already showed that the functionalized optical fiber ball resonators ability to detect CD44 at the attomolar level. The study was in a static condition; repeatability and specificity tests were also performed [28].

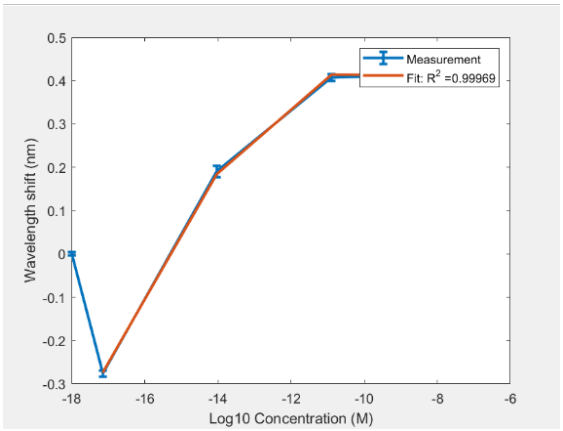

Figure 17. Dynamic CD44 detection with 497-492 μm optical fiber ball resonator biosensor.

During the dynamic measurement of CD44 with 497-492 μm optical fiber ball resonator biosensor, there was a concentration-dependent increase, shown in **Figure 17.** The first measurement was serum; the wavelength shift was observed between the first concentration 7.1 aM and last concentration 16.7 nM. During the dynamic CD44 measurement of another sensor with a diameter of 491-485 μm**,** there was a concentration-dependent RI change, shown in **Figure 18.** The results of the specificity test, both with gamma globulin and Thrombin presented very low change in intesity, it is shown in **Figure 19** and **Figure 20.**

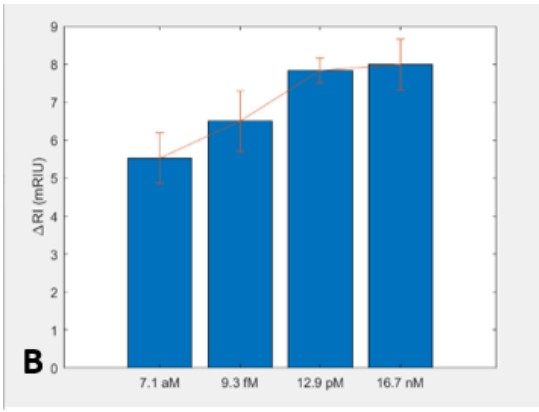

Figure 18. Dynamic CD44 detection with 491-485 µm optical fiber ball resonator biosensor.

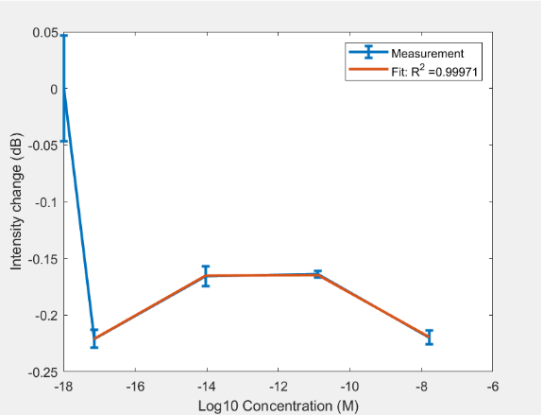

Figure 19. Specificity test done using Thrombin with 485-491 µm optical fiber ball resonator biosensor.

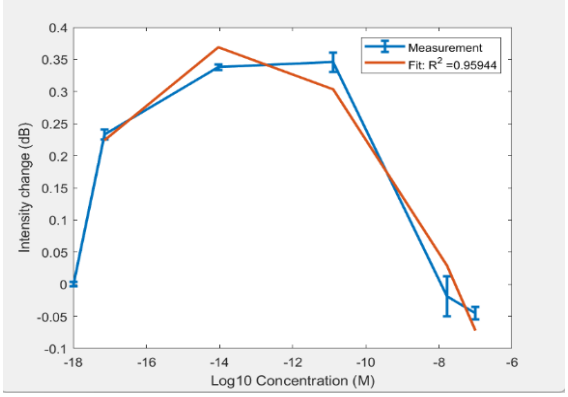

Figure 20. The specificity test was done using gamma-globulin with a 496-491 µm optical fiber ball resonator biosensor.

In order to demonstrate the pressure insensitivity, the pressure characterization of the optical fiber ball resonator sensor with a diameter of 499-494 μm was measured at different depths of water. A sensor was measured at the following depths, 13.6 cm, 16 cm, 26 cm, 36cm, 46cm, 56cm, 66 cm, corresponding to 9.9 mmHg, 11.73 mmHg, 19.07 mmHg, 26.4 mmHg, 33.74 mmHg, 41,07 mmHg, 48.4 mmHg respectively. **Figure 17** shows that the optical fiber ball resonator was not sensitive to the change in pressure. The dynamic measurement was intended to mimic blood flow, where blood pressure is also present. There was a necessity to perform pressure characterization to ensure the sensor was not sensitive to pressure.

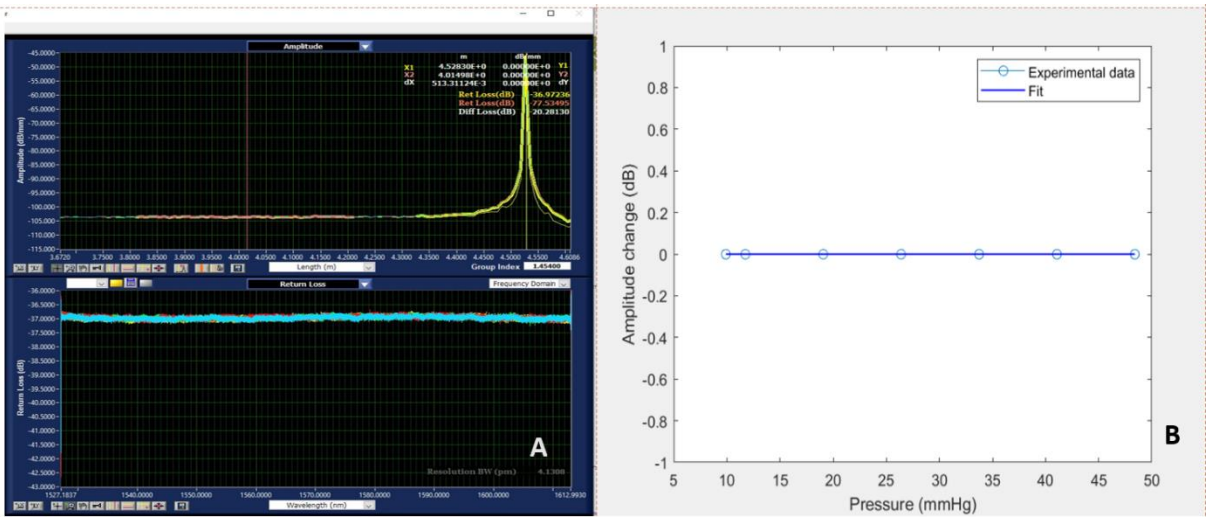

Figure 21. The pressure characterization of ball resonator with a diameter of 499-494 μm (A). MatLab analysis of the pressure characterization measurement.

Atomic force microscope (AFM) is one type scanning probe microscope (SPM) which is based on the change of the interaction force between the sample and a cantilever, a probe with a tip in the end, which deflects as it interacts with the sample surface [30]. This allows to use AFM to study surface morphology and different properties of the surface. Depending on the radius of the AFM probe tip, the resulting image resolution can be down to atomic level. It is possible to study such properties of the sample as elasticity, deformation, adhesion, energy dissipation [31].

In this Thesis, NanoWizard 4 XP BioScience was used to study surface morphology at each stage of functionalization of sensors. NanoWizard is a new AFM device which combines atomic resolution and fast scan (150 lines/sec) with a large scan range (100µm). It can be used to study in long-term experiments providing superb mechanical and thermal stability on inverted microscope. The range of samples that can be studied by this instrument are huge: from single molecules to living cells and even tissues.

AFM height images and 3D images of sensors at different stages of functionalization are shown in **Figures 22 and 23**. As we can see from the images, the surface morphology changes with each surface treatment. **Table 4** shows the results of measurements of height and Roughness of the sensors with different treatment. Surface becomes rougher after silanization with APTMS. The surface become smoother after treatment with GA as was also observed by Shaimi et al [32] .GA is a cross-linker that is frequently used in functionalization; it bind amino groups of APTMS present on the surface with one end and with exposed amines (e.g. from lysines of protein, in our of antibodies) of the ligand [33] . After immobilizing CD44 antibodies on the sensor surface, non-specific sites were blocked with m-PEG-amine which attaches with its amine group on the surface while exposing unreactive methoxy group.

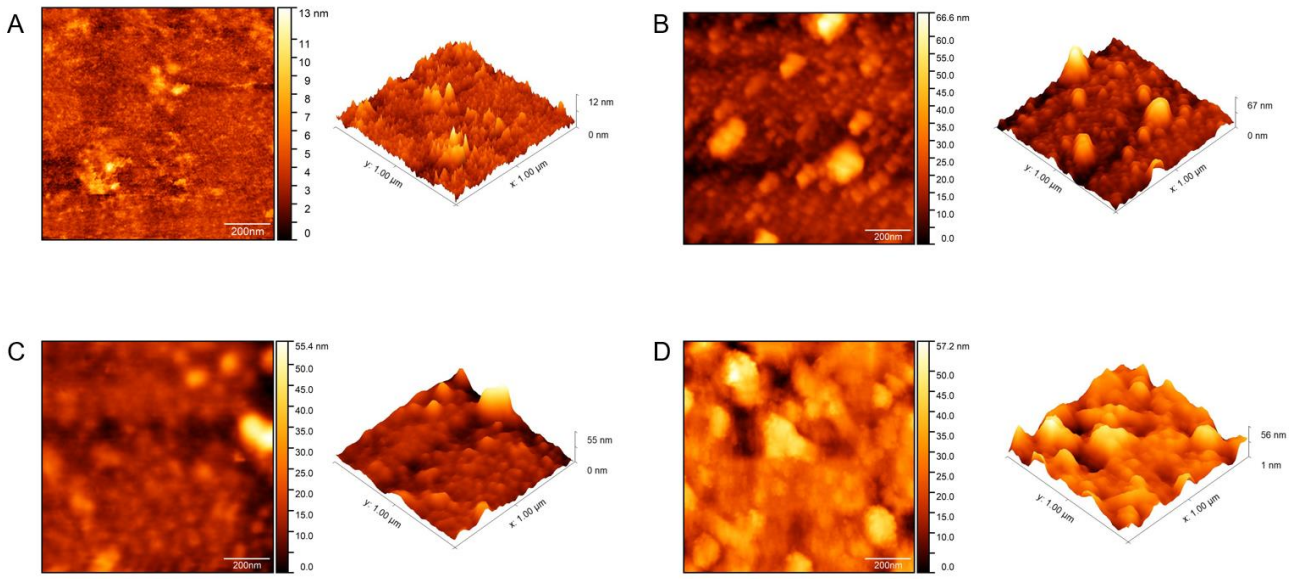

Figure 22. AFM height images and 3D images of sensors at different stages of functionalization. After treatment in Piranha solution (A), APTMS (B), Heat treatment after APTMS (C), Glutaraldehyde (D).

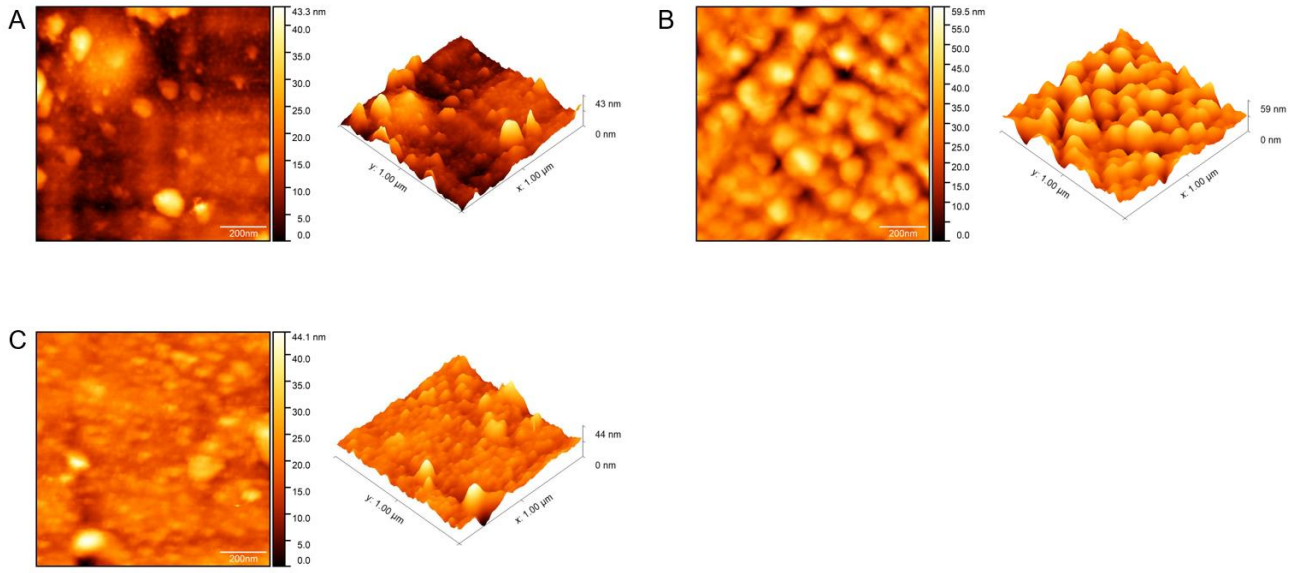

Figure 23. AFM height images and 3D images of sensors at different stages of functionalization. After incubation with Antibodies (A), m-PEG-silane for blocking (B), CD44 detected ball resonator (C).

Table 4. Height and Roughness of the sensors with different treatment

Treatment	Piranha	APTMS	Heat	GA	Ab	mPEG	Ball resonator
Height, nm	18.97±1.164	60.36±4.947	61.50±3.16	58.86±3.24	40.24±2.67	54.45±2.56	51.45±3.65
RMS roughness, nm	1.531±0.124	7.224±0.624	8.468±0.50	6.774±0.51	4.703±0.35	7.824±1.03	6.197±0.56

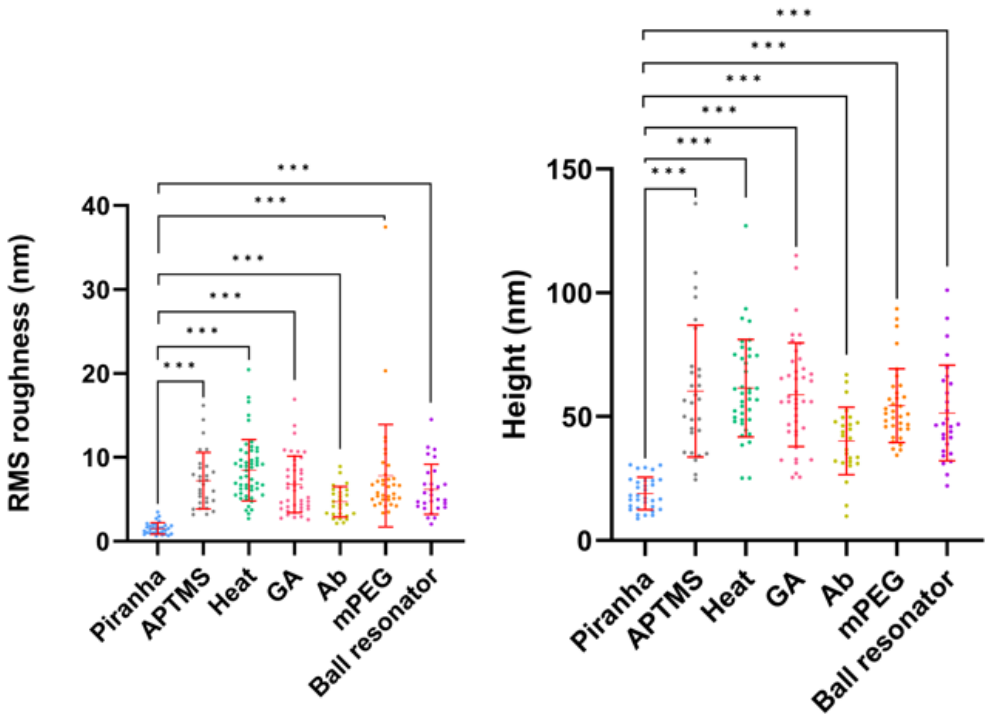

Figure 24. Height and Roughness of the sensors with different treatment derived from Table 4.

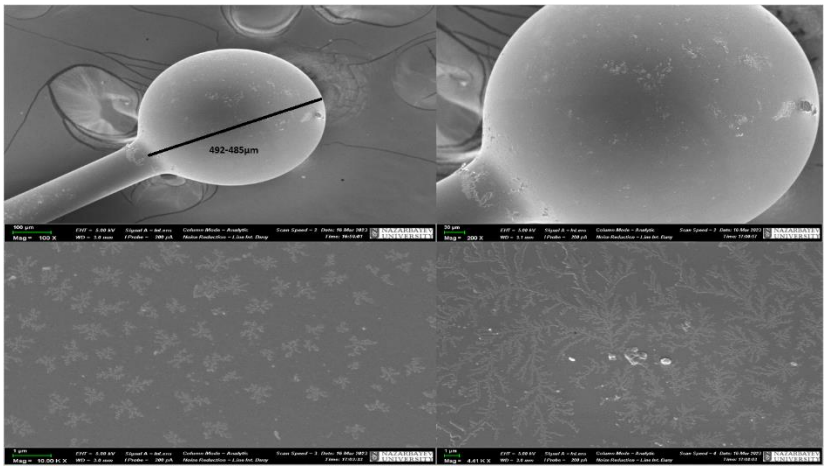

Figure 25. SEM image of functionalized ball resonator diameter of 492-485um.

Chapter 5 – Conclusions

The primary objective of this research is to develop an accurate biosensing platform that detects the cancer biomarker CD44 in a dynamic scenario utilizing a laboratory-fabricated fiber optic sensor that is inexpensive and easy to fabricate. Optical fiber is inexpensive because it is fabricated from a cheap material, SMF-28, used in telecommunication. The manufacturing process is fast and robust, lasting for 5 minutes. This study was focused on moving one step closer to clinical application by mimicking blood flow. *In vitro* studies that imitated the blood flow showed that optical fiber biosensor was able to detect CD44. In the analysis of CD44 at various concentrations, a wavelength shift increased with increasing concentrations of the analyte. A pressure characterization study concluded that the developed optical fiber biosensor is not pressure-sensitive. The optical fiber ball resonator biosensor was used to measure the concentrations of two control proteins, thrombin and gamma-globulin, resulting in no significant change to the obtained signal.

BIBLIOGRAPHY

[1] A. Faber *et al.*, “CD44 as a stem cell marker in head and neck squamous cell carcinoma,” *Oncology Reports*, vol. 26, no. 2. pp. 321–326, 2011, doi: 10.3892/or.2011.1322.

[2] N. S. Basakran, “CD44 as a potential diagnostic tumor marker,” *Saudi Medical Journal*, vol. 36, no. 3. pp. 273–279, 2015, doi: 10.15537/smj.2015.3.9622.

[3] H. Xu, M. Niu, X. Yuan, K. Wu, and A. Liu, “CD44 as a tumor biomarker and therapeutic target,” *Exp. Hematol. Oncol.*, vol. 9, no. 1, pp. 1–14, 2020, doi: 10.1186/s40164-020-00192-0.

[4] Y. Yan, X. Zuo, and D. Wei, “Concise Review: Emerging Role of CD44 in Cancer Stem Cells: A Promising Biomarker and Therapeutic Target,” *Stem Cells Transl. Med.*, vol. 4, no. 9, pp. 1033–1043, 2015, doi: 10.5966/sctm.2015-0048.

[5] C. Chen, S. Zhao, A. Karnad, and J. W. Freeman, “The biology and role of CD44 in cancer progression: Therapeutic implications,” *J. Hematol. Oncol.*, vol. 11, no. 1, pp. 1–23, 2018, doi: 10.1186/s13045-018-0605-5.

[6] B. Fan *et al.*, “Photoelectrochemical Biosensor for Sensitive Detection of Soluble CD44 Based on the Facile Construction of a Poly(ethylene glycol)/Hyaluronic Acid Hybrid Antifouling Interface,” *ACS Appl. Mater. Interfaces*, vol. 11, no. 27, pp. 24764–24770, 2019, doi: 10.1021/acsami.9b06937.

[7] S. Seyedmajidi *et al.*, “Comparison of salivary and serum soluble CD44 levels between patients with oral SCC and healthy controls,” *Asian Pacific J. Cancer Prev.*, vol. 19, no. 11, pp. 3059–3063, 2018, doi: 10.31557/APJCP.2018.19.11.3059.

[8] Y. Xie *et al.*, “A Novel Electrochemical Microfluidic Chip Combined with Multiple Biomarkers for Early Diagnosis of Gastric Cancer,” *Nanoscale Res. Lett.*, vol. 10, no. 1, pp. 1–9, 2015, doi: 10.1186/s11671-015-1153-3.

[9] H. Sung *et al.*, “Global Cancer Statistics 2020: GLOBOCAN Estimates of Incidence and Mortality Worldwide for 36 Cancers in 185 Countries,” *CA. Cancer J. Clin.*, vol. 71, no. 3, pp. 209–249, 2021, doi: 10.3322/caac.21660.

[10] 28.02.2023, “Official information resource of the Prime Minister of the Republic of Kazakhstan.” [Online]. Available: https://primeminister.kz/ru/news/v-kazakhstane-za-poslednie-20-let-smertnost-ot-onkologicheskikh-zabolevaniy-snizilas-na-33-23189#:~:text=«В стране онкологические заболевания занимают,Ежегодно выявляется более 37 тыс.

[11] M. Wang, Y. Xiao, L. Lin, X. Zhu, L. Du, and X. Shi, “A Microfluidic Chip Integrated with Hyaluronic Acid-Functionalized Electrospun Chitosan Nanofibers for Specific Capture and Nondestructive Release of CD44-Overexpressing Circulating Tumor Cells,” *Bioconjug. Chem.*, vol. 29, no. 4, pp. 1081–1090, 2018, doi: 10.1021/acs.bioconjchem.7b00747.

[12] W. Arber, *Current topics in microbiology and immunology*, vol. 6, no. 2. 1977.

[13] L. T. Senbanjo and M. A. Chellaiah, “CD44: A multifunctional cell surface adhesion receptor is a regulator of progression and metastasis of cancer cells,” *Front. Cell Dev. Biol.*, vol. 5, no. MAR, 2017, doi: 10.3389/fcell.2017.00018.

[14] J. Cichy and E. Puré, “The liberation of CD44,” *J. Cell Biol.*, vol. 161, no. 5, pp. 839–843, 2003, doi: 10.1083/jcb.200302098.

[15] L. M. Negi, S. Talegaonkar, M. Jaggi, F. J. Ahmad, Z. Iqbal, and R. K. Khar, “Role of CD44

in tumour progression and strategies for targeting," *J. Drug Target.*, vol. 20, no. 7, pp. 561–573, 2012, doi: 10.3109/1061186X.2012.702767.

[16] K. Range, D. M, and Y. A. Moser, "基因的改变NIH Public Access," *Bone*, vol. 23, no. 1, pp. 1–7, 2012, doi: 10.1038/jid.2009.13.Shedding.

[17] O. Nagano and H. Saya, "Mechanism and biological significance of CD44 cleavage," *Cancer Sci.*, vol. 95, no. 12, pp. 930–935, 2004, doi: 10.1111/j.1349-7006.2004.tb03179.x.

[18] A. G. Zeimet *et al.*, "High serum levels of soluble CD44 variant isoform v5 are associated with favourable clinical outcome in ovarian cancer," *Br. J. Cancer*, vol. 76, no. 12, pp. 1646–1651, 1997, doi: 10.1038/bjc.1997.611.

[19] X. Wang and D. Jin, "Potential Use of Soluble CD44 in Serum as Indicator of T\imor Burden and Metastasis in Patients with Gastric or Colon Cancer," *Cancer Res.*, vol. 54, no. 2, pp. 422–426, 1994.

[20] F. A. Siebzehnrubl, *Proteoglycans in Glioma Stem Cells*. 2021.

[21] S. Dasari, W. Rajendra, and L. Valluru, "Evaluation of soluble CD44 protein marker to distinguish the premalignant and malignant carcinoma cases in cervical cancer patients," *Med. Oncol.*, vol. 31, no. 9, pp. 1–7, 2014, doi: 10.1007/s12032-014-0139-9.

[22] "Breast cancer stem cell markers CD44 and ALDH1A1 in serum.pdf." .

[23] J. Chen, J. Zhou, J. Lu, H. Xiong, X. Shi, and L. Gong, "Significance of CD44 expression in head and neck cancer: A systemic review and meta-analysis," *BMC Cancer*, vol. 14, no. 1, pp. 1–9, 2014, doi: 10.1186/1471-2407-14-15.

[24] Z. Wang *et al.*, "The prognostic and clinical value of CD44 in colorectal cancer: A meta-analysis," *Front. Oncol.*, vol. 9, no. APR, pp. 1–11, 2019, doi: 10.3389/fonc.2019.00309.

[25] H. Emich, D. Chapireau, I. Hutchison, and I. Mackenzie, "The potential of CD44 as a diagnostic and prognostic tool in oral cancer," *J. Oral Pathol. Med.*, vol. 44, no. 6, pp. 393–400, 2015, doi: 10.1111/jop.12308.

[26] I. Čēma, M. Dzudzilo, R. Kleina, I. Franckevica, and Š. Svirskis, "Correlation of soluble cd44 expression in saliva and cd44 protein in oral leukoplakia tissues," *Cancers (Basel).*, vol. 13, no. 22, pp. 1–22, 2021, doi: 10.3390/cancers13225739.

[27] M. D. Marazuela and M. C. Moreno-Bondi, "Fiber-optic biosensors - An overview," *Anal. Bioanal. Chem.*, vol. 372, no. 5–6, pp. 664–682, 2002, doi: 10.1007/s00216-002-1235-9.

[28] A. Bekmurzayeva *et al.*, "Label-free fiber-optic spherical tip biosensor to enable picomolar-level detection of CD44 protein," *Sci. Rep.*, vol. 11, no. 1, pp. 1–13, 2021, doi: 10.1038/s41598-021-99099-x.

[29] M. Shaimerdenova, T. Ayupova, A. Bekmurzayeva, M. Sypabekova, Z. Ashikbayeva, and D. Tosi, "Spatial-Division Multiplexing Approach for Simultaneous Detection of Fiber-Optic Ball Resonator Sensors: Applications for Refractometers and Biosensors," *Biosensors*, vol. 12, no. 11, p. 1007, 2022, doi: 10.3390/bios12111007.

[30] Y. Zhou and J. Du, "Atomic force microscopy (AFM) and its applications to bone-related research," *Prog. Biophys. Mol. Biol.*, vol. 176, pp. 52–66, Dec. 2022, doi: 10.1016/j.pbiomolbio.2022.10.002.

[31] S. R. Falsafi, H. Rostamabadi, E. Assadpour, and S. M. Jafari, "Morphology and microstructural analysis of bioactive-loaded micro/nanocarriers via microscopy techniques; CLSM/SEM/TEM/AFM," *Adv. Colloid Interface Sci.*, vol. 280, 2020, doi: 10.1016/j.cis.2020.102166.

[32] R. Shaimi and S. C. Low, "Prolonged protein immobilization of biosensor by chemically cross-linked glutaraldehyde on mixed cellulose membrane," *J. Polym. Eng.*, vol. 36, no. 7,

pp. 655–661, 2016, doi: 10.1515/polyeng-2015-0308.

[33] M. P. Nicholas, L. Rao, and A. Gennerich, *Covalent immobilization of microtubules on glass surfaces for molecular motor force measurements and other single-molecule assays*, vol. 1136. 2014.